

Book of Tutorials and Abstracts



European Microbeam Analysis Society

EMAS 2011

**12th
EUROPEAN WORKSHOP**

on

MODERN DEVELOPMENTS AND APPLICATIONS IN MICROBEAM ANALYSIS

15 to 19 May 2011
at the
Centre de Congrès d'Angers
Angers, France

Organised in collaboration with
GN-MEBA - Groupement National de Microscopie
Électronique à Balayage et de microAnalyses



QUANTITATIVE MICROSTRUCTURAL ANALYSIS BY ORIENTATION CONTRAST MICROSCOPY

Leo A.I. Kestens^{1,2}, R. Decoeker¹ and R.H. Petrov^{1,2}

- 1 Ghent University, Materials Engineering Department
Technologiepark 903, BE-9052 Gent, Belgium
e-mail: leo.kestens@ugent.be
- 2 Delft University of Technology, Materials Engineering
Mekelweg 2, NL-2628 CD Delft, The Netherlands

Leo Kestens was born on June 26th 1964 in Aalst, Belgium. More than twenty years ago he graduated as an Engineer in Physics from Ghent University in Belgium. From Ghent he moved to Leuven where he has made the switch from physics to materials science and obtained his Ph.D. in 1994 with a dissertation on the role of crystallographic textures in electrical steels, which are used as magnetic flux carriers in a wide variety of applications. After his promotion he has continued his research in the field of steel metallurgy, first as a post-doc in the group of Prof. John J. Jonas at McGill University in Montreal and afterwards at the Centre for Research in Metallurgy (CRM) in Ghent. In 1998 he returned to Ghent University where he has started his own research group on the crystallographic aspects of physical metallurgy. In 2005 he was appointed at Delft University of Technology (TU Delft) where he occupied the chair on Microstructure Control in Metals in the Materials Science and Engineering Department. In 2009 he returned to Ghent University with an FWO-Odyseus grant that allowed him to set up a research group with currently 12 research scientists.

Orientation contrast microscopy is a technique of image reconstruction based on local identification of crystal phase and crystal orientation. Before describing the details of the technique itself a number of crystallographic tools are introduced that allow converting crystallographic data to image information. The present paper emphasizes on the precise crystallographic derivation of the crystal orientation from the Kikuchi diffraction pattern.

1. INTRODUCTION OF A SAMPLE REFERENCE SYSTEM

In general, a macroscopic material volume of a commercially manufactured material is not a single crystal but a polycrystalline aggregate, i.e., it consists of many different single crystals, each with their own orientation in space. In order to characterize the presence of crystal orientations a sample reference system is introduced. For rolled material this is done as illustrated in Fig. 1. The X-axis corresponds to the rolling direction (RD), the Z-axis coincides with the plane normal (ND), i.e., the direction perpendicular to the rolled sheet, and the Y-axis is defined in the plane of the sheet so that X, Y and Z constitute an orthogonal right-handed coordinate system. The obtained Y-axis is denominated as the transverse direction (TD) and points from the reader towards the sheet.

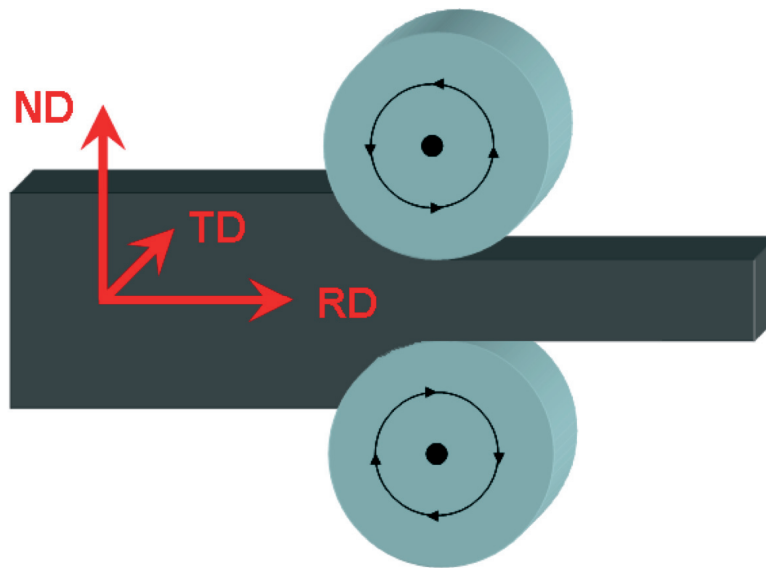


Figure 1. Definition of a sample reference system for the example of a rolled sheet.

The rolling direction is uniquely defined but the normal axis can be chosen pointing upwards or downwards. Choosing the normal direction pointing downwards will also invert the direction of the transverse direction, in order to maintain a right-handed axis system. This will, however, have no effect on the representation of crystal orientation because of inherent sample symmetry.

2. DESCRIPTION OF THE ORIENTATION OF A SINGLE CRYSTAL

The orientation of each single crystal is described by the orientation relationship between the sample reference system K_S , as introduced in the previous section, and the crystal reference system K_C which is associated with the crystallographic $\langle 100 \rangle$ directions of the crystal, cf. Fig. 2 (example for a cubic crystal). The orientation relation between two reference systems is uniquely defined by three degrees of freedom. To describe this orientation relation, several representations are used such as the orientation matrix, the Miller indices and the Euler angles.

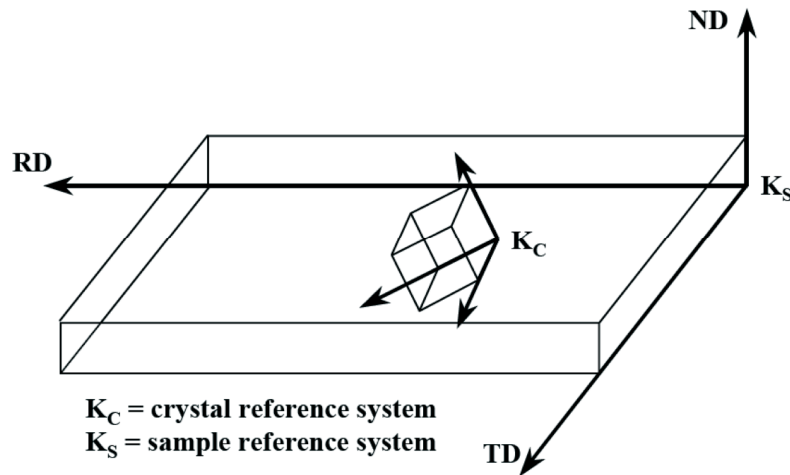


Figure 2. The orientation of a crystal is described by the orientation relation between the sample reference system K_S and the crystal reference system K_C .

2.1. The orientation matrix $[g]$

The orientation matrix $[g]$ is the matrix that describes the transformation of the sample reference system to the crystal reference system. This is expressed in the following equation, which expresses the transformation of the coordinates of an arbitrary vector \mathbf{r} from the sample to the crystal reference system:

$$\mathbf{r}_c = [g]\mathbf{r}_s \quad (1).$$

The 9 components of the matrix are defined by the direction cosines between the axes of the sample and the crystal reference system, as indicated in Fig. 3. When the angles between the X-, Y- and Z-axis of the crystal reference system and the three corresponding axes of the sample reference system are denominated by $\alpha_1, \beta_1, \gamma_1$; $\alpha_2, \beta_2, \gamma_2$ and $\alpha_3, \beta_3, \gamma_3$ respectively, then the transformation matrix is given by:

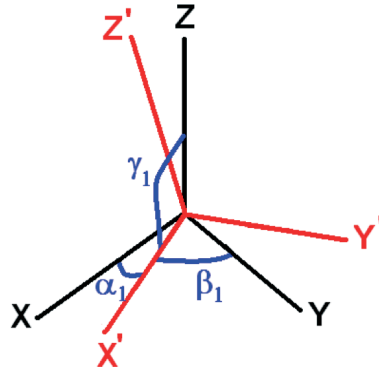


Figure 3. The angles between K_C and K_S .

$$[g] = \begin{pmatrix} \cos \alpha_1 \cos \beta_1 \cos \gamma_1 \\ \cos \alpha_2 \cos \beta_2 \cos \gamma_2 \\ \cos \alpha_3 \cos \beta_3 \cos \gamma_3 \end{pmatrix} \quad (2).$$

Because the matrix has nine components for only three degrees of freedom, six additional relations between the different components must be valid. Since the rows of Eq. 2 are the unit vectors of K_C , expressed in the frame K_S , the following orthonormality conditions hold:

$$\sum_{k=1}^3 g_{ki} g_{kj} = \delta_{ij} \quad i, j = 1 \rightarrow 3 \quad (3).$$

The columns of Eq. 2, on the other hand, are the unit vectors of K_S , described in the reference frame K_C , and therefore the following orthonormality conditions are also valid:

$$\sum_{k=1}^3 g_{ik} g_{jk} = \delta_{ij} \quad i, j = 1 \rightarrow 3 \quad (4)$$

with δ_{ij} the well-known Kronecker delta ($\delta_{ij} = 1$ if $i=j$ and $\delta_{ij} = 0$ if $i \neq j$).

2.2. Miller indices

When using Miller indices, an orientation is characterized by the crystallographic plane (hkl) which is parallel to the XY -plane of the sample (e.g., the rolling plane) and by the crystal direction $[uvw]$ that is parallel to the X -axis of the sample (e.g., the rolling direction). It is self-evident that, when dealing with cubic materials, this also implies that the direction $[hkl]$ is parallel to the normal of the rolling plane. The use of Miller indices is illustrated in Fig. 4 for the crystal orientation, which is described by the indices $(110)[001]$. Also in this case the six parameters that are used only display three degrees of freedom since both the plane and the

direction are uniquely determined by unit vectors $[h'k'l']$ and $[u'v'w']$ and because the direction $[uvw]$ needs to be coplanar with the plane (hkl) it entails $u.h+v.k+w.l = 0$. It implies that the Miller indices $(hkl)[uvw]$ comply with 3 equations and thus, only 3 degrees of freedom remain.

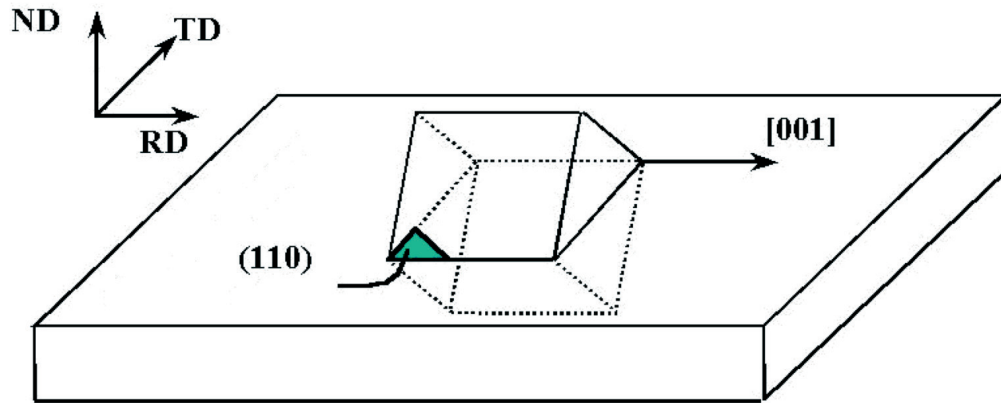


Figure 4. Miller indices representation of the Goss orientation $(110)[001]$.

2.3. Euler angles

According to Euler's rotation theorem, any rotation may be described using three angles, which are conventionally called the Euler angles. An arbitrary rotation A of a reference system can therefore be characterized by three angles for whom the associated transformations are identified by the matrices B , C and D . The overall transformation can thus be performed by applying the three *partial* transformations consecutively:

$$[g] = B.C.D \quad (5).$$

In quantitative texture analysis, several conventions are used for the definition of the Euler angles. The most widely accepted one was introduced by Bunge [1]. For the transformation of the crystal axis system (x,y,z) into the sample reference system (X,Y,Z) which is described by the Euler angles $(\varphi_1, \Phi, \varphi_2)$, the first rotation is performed over an angle φ_1 around the z -axis, the second over an angle Φ around the x' -axis (i.e., the new x -axis), and the third over an angle φ_2 around the z'' -axis, as presented in Fig. 5.

The partial transformations are thus given by:

$$B = \begin{pmatrix} \cos \varphi_2 & \sin \varphi_2 & 0 \\ -\sin \varphi_2 & \cos \varphi_2 & 0 \\ 0 & 0 & 1 \end{pmatrix}; \quad C = \begin{pmatrix} 1 & 0 & 0 \\ 0 & \cos \Phi & \sin \Phi \\ 0 & -\sin \Phi & \cos \Phi \end{pmatrix}; \quad D = \begin{pmatrix} \cos \varphi_1 & \sin \varphi_1 & 0 \\ -\sin \varphi_1 & \cos \varphi_1 & 0 \\ 0 & 0 & 1 \end{pmatrix} \quad (6).$$

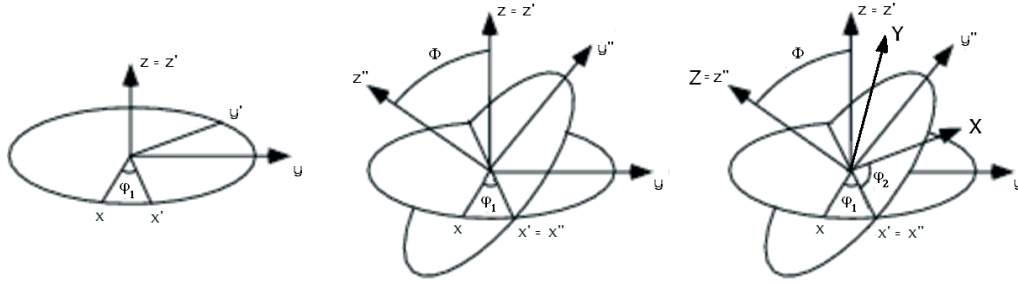


Figure 5. Euler angles according to the Bunge convention.

Hence, the orientation matrix $[g]$ can be expressed in function of the Euler angles $(\varphi_1, \Phi, \varphi_2)$:

$$[g] = \begin{bmatrix} (\cos \varphi_1 \cos \varphi_2 - \sin \varphi_1 \sin \varphi_2 \cos \Phi)(\sin \varphi_1 \cos \varphi_2 - \cos \varphi_1 \sin \varphi_2 \cos \Phi)(\sin \varphi_2 \sin \Phi) \\ (-\cos \varphi_1 \sin \varphi_2 - \sin \varphi_1 \cos \varphi_2 \cos \Phi)(-\sin \varphi_1 \sin \varphi_2 + \cos \varphi_1 \cos \varphi_2 \cos \Phi)(\cos \varphi_2 \sin \Phi) \\ (\sin \varphi_1 \sin \Phi)(-\cos \varphi_1 \sin \Phi)(\cos \Phi) \end{bmatrix} \quad (7).$$

Because of the cyclic nature of angular rotations, any orientation in space can be represented with Euler angles confined within the following range:

$$0 \leq \varphi_1, \varphi_2 \leq 2\pi \text{ and } 0 \leq \Phi \leq \pi.$$

3. OIM[®]: AN AUTOMATED EBSD MEASURING TECHNIQUE

Crystallographic texture data can be obtained in several ways e.g., by X-ray diffraction (XRD), neutron diffraction (ND), electron backscatter diffraction (EBSD), or selected area diffraction in a transmission electron microscope (TEM). Here *orientation-imaging microscopy* (OIM) will be considered, which is an automated measuring technique based on EBSD. The main advantage of this technique is the possibility to gather local crystal orientation information on a much larger scale. XRD and ND measure the texture in an area of several mm² but no microstructural details can be obtained from these techniques. TEM, on the other hand, covers the higher end of the resolution spectrum but it only probes a limited surface area and thus entails inherently poor data statistics. The EBSD process and the OIM technique will therefore be explained in more detail in the following section.

3.1. Electron backscatter diffraction (EBSD)

Electron backscatter diffraction (EBSD) is a technique, which allows crystallographic information to be obtained from samples in the scanning electron microscope (SEM). In order

to obtain an EBSD image a stationary electron beam with an acceleration voltage of 20 to 30 kV strikes a tilted crystalline sample (cf. Fig. 6a) and the diffracted electrons form a so-called Kikuchi pattern on a fluorescent phosphor screen, as illustrated in Fig. 6b. This pattern is characteristic of the crystal structure and orientation of the sample volume from which it was generated. The EBSD sample is usually tilted at 70° to the horizontal to optimize both the contrast in the diffraction pattern and the fraction of electrons scattered from the sample. For smaller tilt angles the contrast in the diffraction pattern decreases.

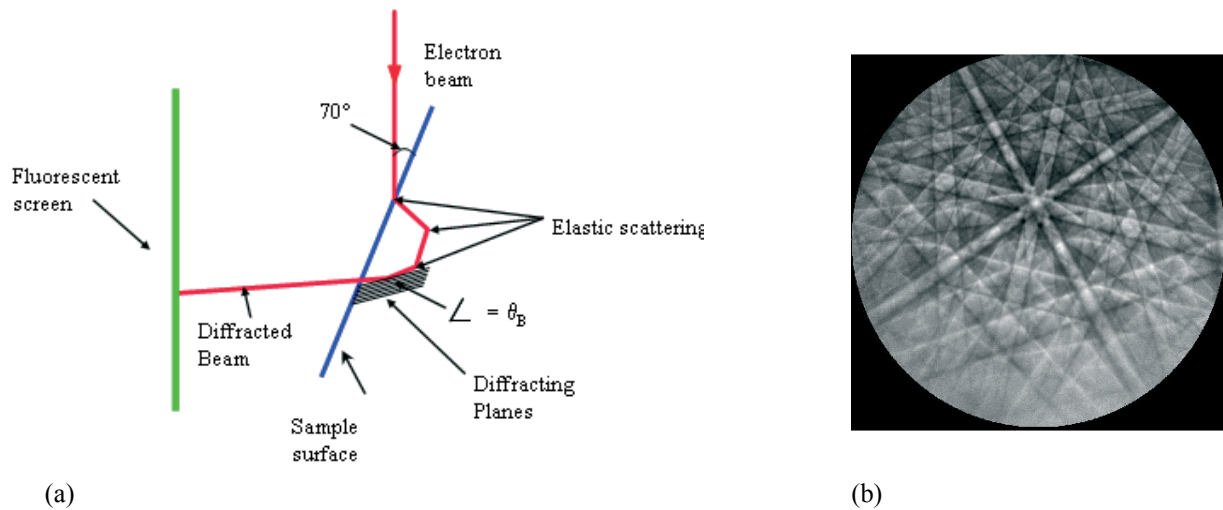


Figure 6. a) Principle of the EBSD phenomenon and measuring technique. b) An example of the obtained Kikuchi pattern.

Due to the small spot size of the electron beam and the limited penetration depth of the backscattered electrons, the technique is, unlike XRD, very sensitive to imperfections of the sample surface and the sample preparation will therefore be of critical importance.

3.2. The physics of electron backscatter diffraction

3.2.1. The formation of the Kikuchi pattern. The formation of the Kikuchi pattern is based on the principle of diffraction. The electron beam collides with the sample and as a result of elastic scattering electrons diverge in all directions from a point just below the sample surface and will impinge upon crystal planes in all directions. Two cones of diffracted electrons are produced, wherever the Bragg condition for diffraction is satisfied by a family of atomic lattice planes in the crystal. The Bragg law for positive interference of the n^{th} order imposes the following condition on the wavelength l of the incident wave, the angle of incidence θ and the distance d between the atom layers:

$$2.d.\sin(\theta) = n.\lambda \quad (8).$$

As can be seen from Fig. 7 the Bragg law demands that the difference in distance travelled by both waves ($2.d.\sin \theta$) is an integer multiple of the wavelength λ .

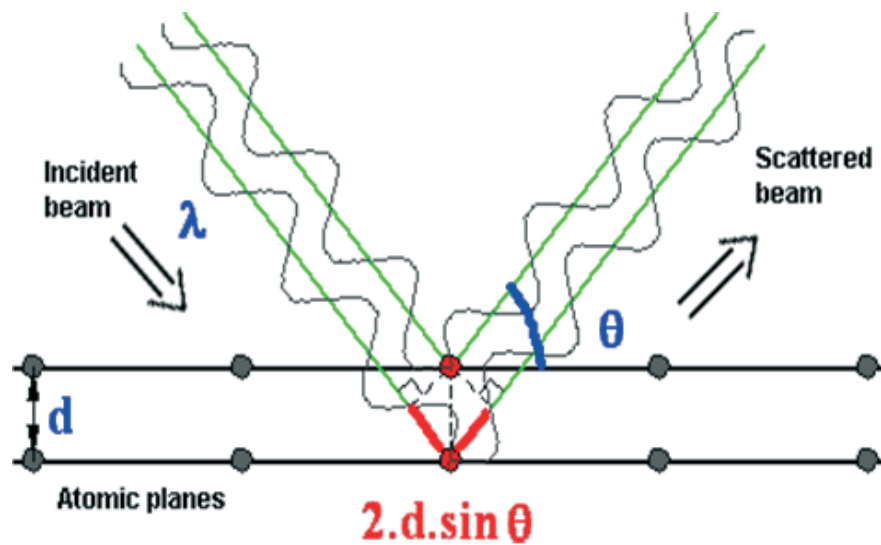


Figure 7. Bragg's law [2].

The fraction of the electrons that meet the Bragg condition for the encountered crystallographic plane will be diffracted into diffraction cones as shown in Fig. 8 [3]. Due to the acceleration voltage of 30 kV in the SEM, the de Broglie wavelength of the electrons is around 0.007 nm and the diffraction angle θ is around 1.4° . The cones therefore intersect the phosphor screen as nearly straight lines and the bands can therefore be considered as a prolongation of the diffracting plane emerging from the crystal lattice. These cones are produced for each family of lattice planes and therefore a pattern of intersecting Kikuchi bands is observed on the phosphor screen as observed in Fig. 6b. Only the electrons of the precise energy imposed by the Bragg condition contribute to the observed pattern. This fraction of electrons consists of elastically scattered electrons, the so-called backscattered electrons. Inelastically scattered electrons have lost part of their energy and will produce a diffuse background in the pattern. The pattern is recorded by a sensitive (digital) CCD camera and the information is sent to a PC where EBSD software automatically locates the positions of individual Kikuchi bands.

3.2.2. Identification of the crystallographic plane, related to a set of Kikuchi bands. Since the Kikuchi bands can be considered as the intersection of the diffracting planes and the phosphor screen, it is possible to determine the angle between two planes from their respective Kikuchi lines. This has been illustrated in Fig. 9, which shows two Kikuchi lines arising from different diffracting planes. Since all electrons are backscattered from the point (O) where the beam collides with the sample, the two diffracting planes are fully determined by the sets of non-colinear points (O, P, Q) and (O, R, S), respectively. The normals $\overline{n_1}$ and $\overline{n_2}$ to these planes can be obtained as follows:

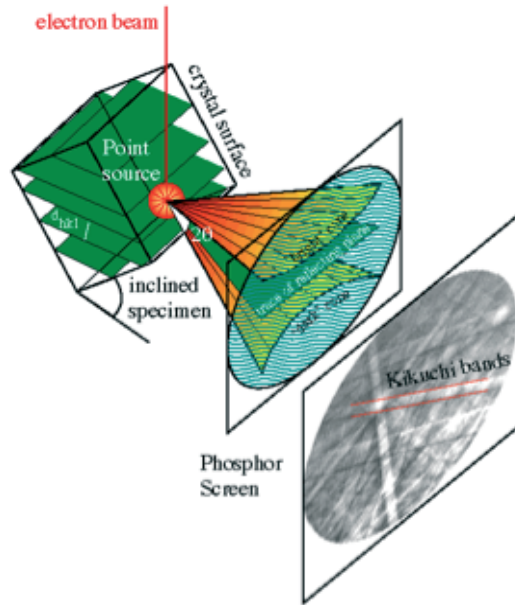


Figure 8. Formation of Kikuchi diffraction patterns.

$$\bar{n}_1 = \frac{\overline{OPxOQ}}{|\overline{OPxOQ}|}$$

$$\bar{n}_2 = \frac{\overline{ORxOS}}{|\overline{ORxOS}|}$$

(9).

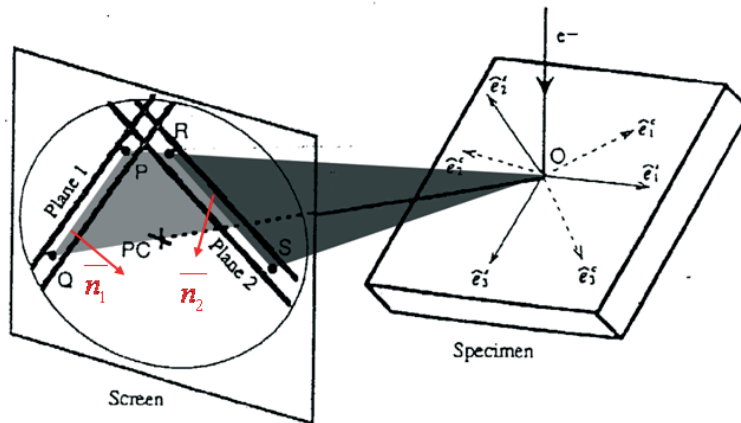


Figure 9. Construction of the diffracting plane normal, based on the Kikuchi line.

The angle between the crystallographic planes, involved can then be determined from the scalar product of the two normal vectors:

$$\cos \gamma = \left| \bar{n}_1 \cdot \bar{n}_2 \right|$$

(10).

The identification of the crystallographic planes, producing the observed bands, is based on the comparison of the measured angles with theoretical angles for the relevant phase, which is a priori provided by the user. E.g., when measuring a cubic crystal structure, an angle of 45° indicates that the diffracting planes are a $\{110\}$ plane and a $\{100\}$ plane. A measured angle of 54° indicates that the Kikuchi lines are arising from a $\{111\}$ plane and a $\{110\}$ plane. It is, however, not possible to determine which line arises from which plane when only two lines are available. Therefore, at least three Kikuchi lines are required to determine which line corresponds to which crystallographic plane.

3.2.3. *Calculation of the crystallographic orientation.* In order to determine the crystallographic orientation, based on the observed Kikuchi pattern, the following four reference systems are introduced:

- a sample reference system (cf. section 1);
- a screen reference system (cf. Fig. 10a);
- a pattern reference system (cf. Fig. 10b);
- a crystal reference system (cf. section 2).

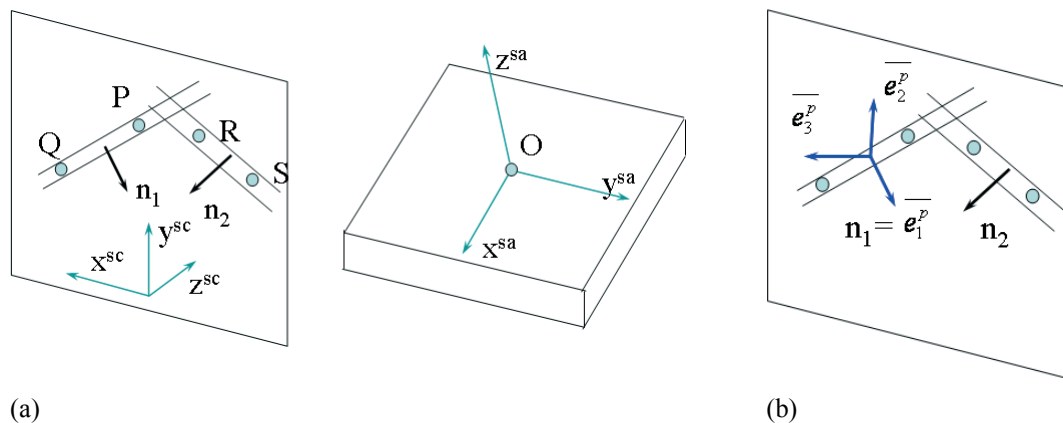


Figure 10. Introduction of (a) the screen reference frame and (b) the pattern reference frame.

For the introduction of the screen reference system, the X- and Y-axes are chosen to collide with the horizontal and vertical direction in the plane of the screen, as shown in Fig. 10a. This implies that the Z-axis is perpendicular to the screen. Unit vectors along these three axes form an orthonormal basis, denoted by e^{sc} .

An orthonormal basis related to the Kikuchi pattern e^p can be defined by employing the normal vectors of the crystal planes (constructed in Eq. 9) as follows:

$$\begin{aligned}
\bar{e}_1^p &= \bar{n}_1 \\
\bar{e}_2^p &= \bar{n}_1 \otimes \bar{n}_2 \\
\bar{e}_3^p &= \bar{e}_1^p \otimes \bar{e}_2^p
\end{aligned}
\tag{11}$$

The resulting orthonormal basis is shown in Fig. 10b.

The three unit vectors of the basis in the sample reference system e^{sa} are chosen, according to Fig. 1, parallel to the rolling, transverse and normal direction, respectively. The basis related to the crystal reference system e^c is formed by the three unit vectors along the crystal directions [100], [010] and [001].

The orientation of a crystal is, by definition, the description of the crystal axes in the sample reference system. This relation is deduced by considering three consecutive transformations. The crystal reference frame will be expressed in terms of the pattern reference frame, which will be expressed in terms of the screen reference system, which in turn, will be expressed in terms of the sample reference system. Combining these three transformations will result in the transformation matrix between the crystal and sample reference system.

Since the construction of the vectors, related to the basis e^p , is based on the known coordinates of points O , P , Q , R and S . The transformation matrix g' from pattern to screen coordinates can therefore be calculated and is given by:

$$g'_{ij} = \bar{e}_i^p \cdot \bar{e}_j^{sc} \tag{12}$$

The transformation from the sample reference system to the screen reference system can be deduced directly from the construction presented in Fig. 11.

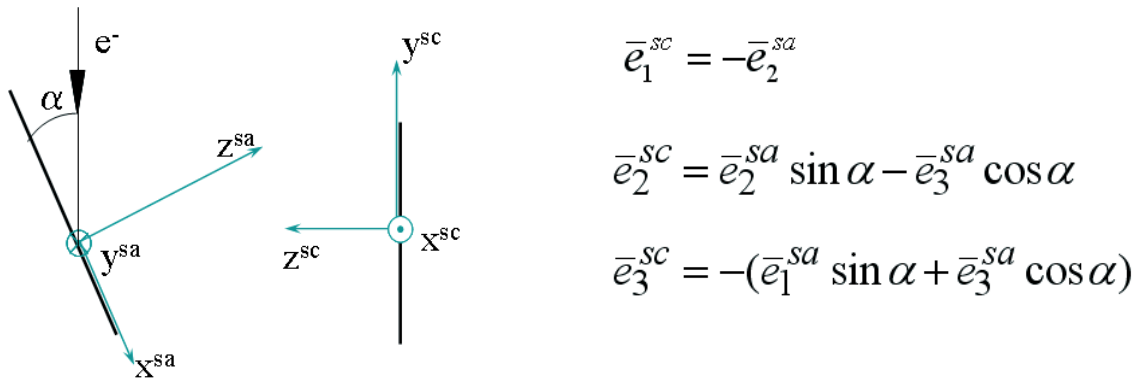


Figure 11. The transformation between the sample reference system and the screen reference system

The transformation matrix g'' from screen to sample coordinates is calculated as follows:

$$g_{ij}'' = \overline{e_i^{sc}} \cdot \overline{e_j^{sa}} \quad (13).$$

Finally the pattern reference system is expressed in terms of the crystal reference system. This can be achieved by expressing the pattern basis vectors in terms of the crystal basis vectors. The first basis vector $\overline{e_1^p}$ was constructed as being the normal to the plane OQP. By employing the procedure as explained in the previous section, the Miller indices of the crystallographic plane involved can be determined. The vector $\overline{e_1^p}$ can therefore also be expressed in terms of the Miller indices:

$$\overline{e_1^p} = \frac{(hkl)_1}{|(hkl)_1|} \quad (14).$$

A similar reasoning, concerning the construction of the vectors $\overline{e_2^p}$ and $\overline{e_3^p}$, leads to the following expressions:

$$\begin{aligned} \overline{e_2^p} &= \frac{(hkl)_1}{|(hkl)_1|} \otimes \frac{(hkl)_2}{|(hkl)_2|} \\ \overline{e_3^p} &= \overline{e_1^p} \otimes \overline{e_2^p} \end{aligned} \quad (15).$$

Since these equations describe the pattern reference system in terms of the crystal reference system, the transformation matrix between the two respective bases can be determined:

$$g_{ij}''' = \overline{e_i^c} \cdot \overline{e_j^p} \quad (16).$$

The transformation matrix between the crystal and the sample reference system, i.e., the orientation matrix of the crystal, can now be calculated by combining the obtained transformation matrices g' , g'' and g''' .

$$g_{ij} = \sum_k \sum_l g'''_{ik} \cdot g'_{kl} \cdot g''_{lj} \quad (17).$$

As explained in the previous section, three sets of Kikuchi bands are required to characterize an orientation. If the captured Kikuchi pattern contains more bands than required (which generally is the case), the orientation is calculated repeatedly. The solution that is obtained most frequently is chosen as the orientation for the measured spot.

4. ORIENTATION IMAGING MICROSCOPY[®] (OIM)

Orientation imaging microscopy[®] (OIM) is a commercial software package from EDAX-TSL which automates the capturing and processing of the EBSD measuring data. The idea is to scan the electron beam on a regular grid across a polycrystalline sample and measure the crystal orientation at each point. The resulting map will then reveal the constituent phase distribution, grain morphology, orientations and boundaries. A typical OIM-setup is presented in Fig. 12.

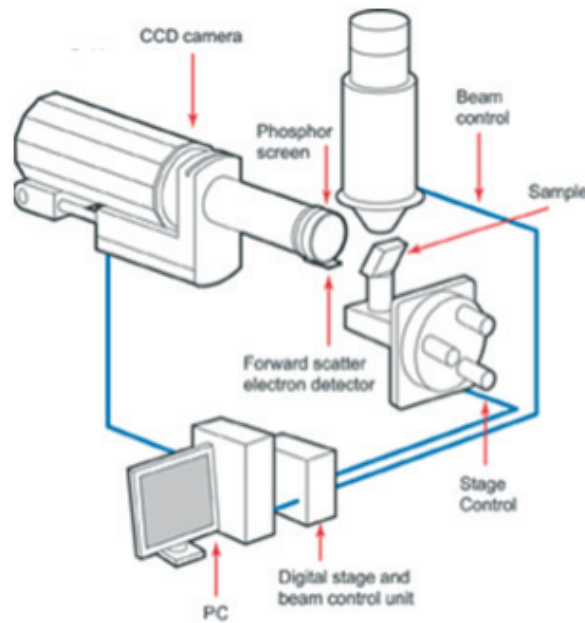


Figure 12. Typical setup for OIM measurements [1].

The electron beam collides with the sample and a Kikuchi pattern is formed on the phosphor screen. This image is recorded by the CCD camera and is sent to the computer, which processes the pattern to determine the crystallographic orientation at the examined spot. Subsequently, the computer sends a signal to the hardware for the beam control which shifts the beam to the next spot of the area under investigation, following a hexagonal or rectangular grid, as shown in Fig. 13. The step size is chosen by the user and is limited by the resolution of the SEM, which is of the order of 0.5 μm for a SEM with W-filament but approximately 0.1 μm for a SEM with FEG filament (the operating conditions that apply to EBSD do not allow to obtain the optimum spatial resolution of conventional secondary electron image mode).

Using the post-processing software a wide variety of quantitative data can be obtained from the collected crystallographic information such as texture plots (ODF, arbitrary pole figures and

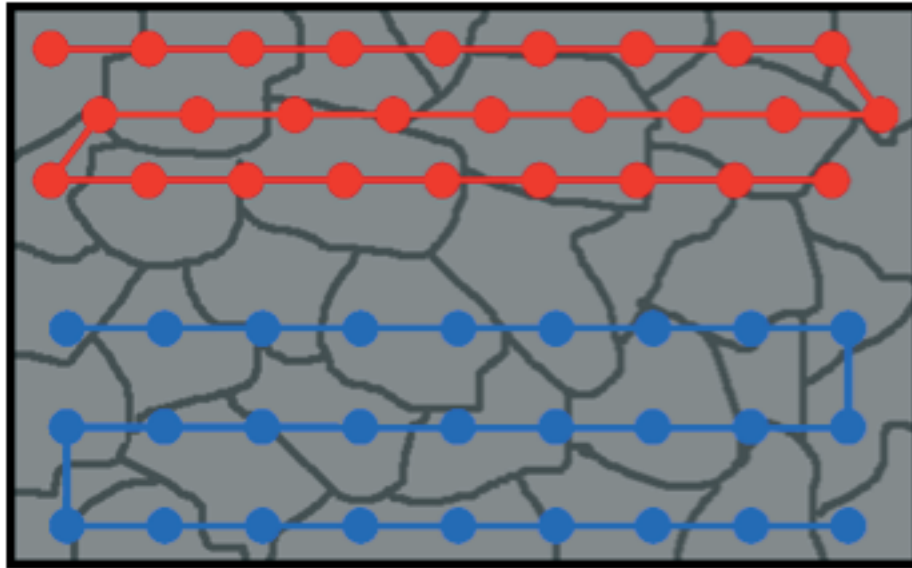


Figure 13. Hexagonal (red) or rectangular (blue) scanning grid of the electron beam in OIM.

inverse pole figures), grain size distributions, misorientation profiles, etc. An example of an ND inverse pole figure map is shown in Fig. 14. Each point is coloured, according to the coded unit triangle of the ND inverse pole figure; e.g., all grains that have a $[111]$ -direction parallel to the ND are coloured blue. Fig. 14c shows the grain size distribution that was derived from the orientation contrast map of Fig. 14a.

From the Kikuchi pattern, two additional parameters can be derived, namely the image quality (IQ) and the confidence index (CI). The image quality parameter quantifies the sharpness of the contrast of an electron backscatter diffraction pattern and can directly be related to the presence of defects in the crystal lattice in the examined region. This parameter depends on the material under investigation but is nearly independent of the crystal orientation. This allows several microstructural features to be distinguished on a map, using the image quality value as a gray scale legend, i.e., a light region indicates a high IQ while a dark region corresponds to low IQ-values. An example of such a map is shown in Fig. 15. The grain boundaries can be seen clearly on such a map since the lattice displays considerable lattice imperfections in the grain boundary area, which results in a lower IQ. As the material that is shown in Fig. 15 is a slightly deformed steel sample, it exhibits a substructure composed of dislocation cells and strain heterogeneities. It can be observed that the IQ contrast also reveals these sub-structural elements. Another interesting feature that can be seen is the occurrence of a secondary phase particle in the middle of micrograph, which is presumably a TiN inclusion in this case. A third observation that can be made is the occurrence of a greyscale gradient within the grains, which may be attributed to a local higher dislocation density, which disturbs the perfect lattice.

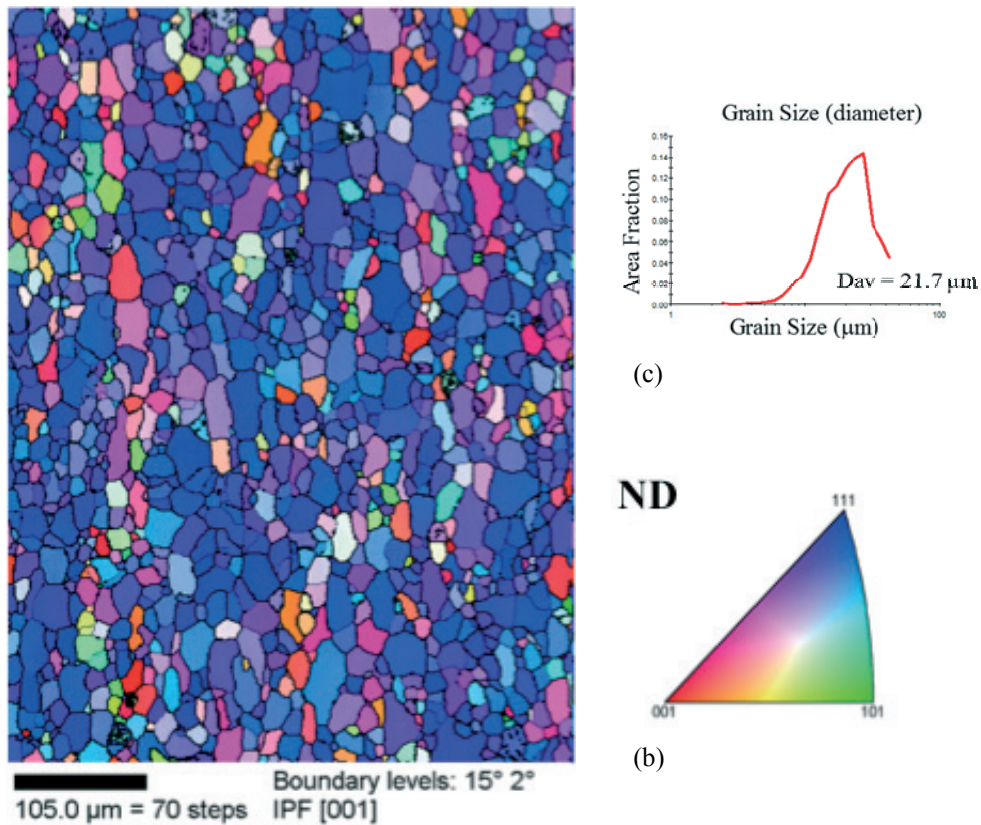


Figure 14. a) Example of an orientation contrast scan. b) Colour code according to standard stereographic triangle. c) Grain size distribution derived from OIM map.

As mentioned before, each set of three Kikuchi bands in the observed pattern can be used to determine the crystallographic orientation. The orientation is determined for all possible sets (N_{Tot}) and the most frequently occurring solution (N_1) is chosen as the effective orientation. The confidence index is then defined as $(N_1 - N_2)/N_{\text{Tot}}$ with N_2 being the number of solutions resulting in the second most frequently obtained orientation. This parameter is often used as a threshold to determine which experimental points can be employed for further processing. The CI is also an important parameter for the *clean-up* methods, provided within the OIM software. These algorithms allow altering the determined orientation and/or phase of single experimental points, based on correlation of its orientation/phase with those of the surrounding points. An example is given in Fig. 16. The centre pixel does not belong to any grain; it has an orientation differing from all surrounding pixels. The clean-up procedure changes the orientation of the pixel to the orientation of the grain that has most neighbouring pixels. If several surrounding grains would have an equal number of pixels adjacent to the one under consideration, one of them is picked at random. Once the dominant neighbouring grain is determined, the orientation of the pixel is changed to match that of the neighbouring pixel of the grain with the highest CI.

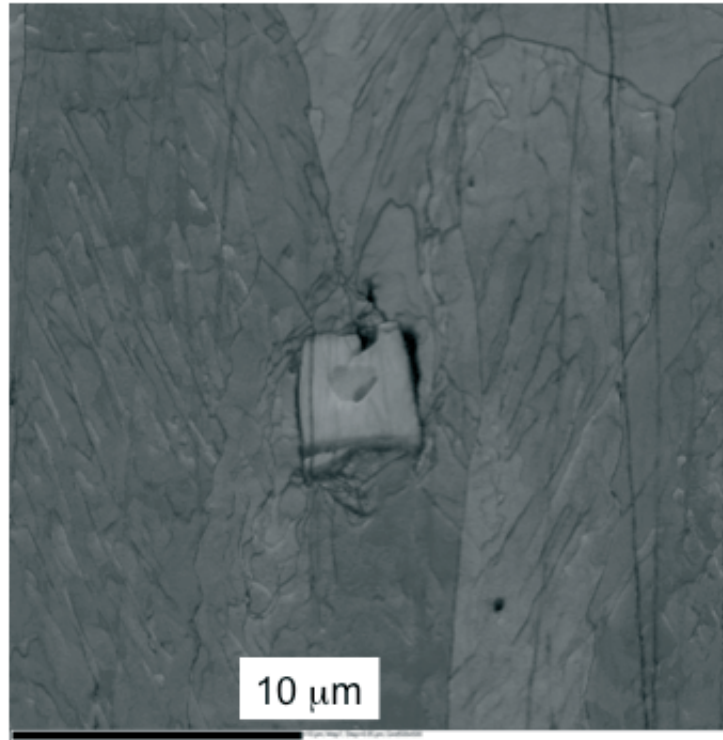


Figure 15. Example of orientation contrast image. Gray scale according to image quality of the Kikuchi pattern.

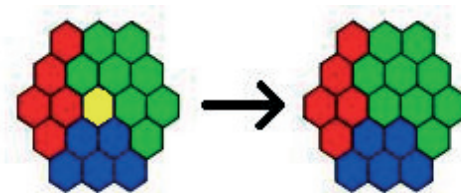


Figure 16. Changing of the measured orientation, based on correlation with the neighbouring points.

Since the orientation of the experimental data is being changed, it is very important to avoid the introduction of artificial trends into the data. These algorithms show best results when the grain size is considerably greater than the step size of the scan.

5. SUMMARY

In the present paper the crystallographic tools were briefly reviewed that are employed (i) to represent crystallographic orientations, and (ii) to reconstruct an image of the microstructure. In orientation contrast microscopy the image data is obtained from electron backscattered

diffraction (EBSD) patterns that are collected by a scanning electron beam over the sample surface. The backscattered electrons are diffracted according to a Kikuchi pattern that is visualized on a phosphorous luminescent screen. The method of pattern indexation and orientation calculation was explained in detail. The orientation contrast image that is reconstructed from the crystallographic data contains quantitative information on the crystal phase and the crystal orientation. By taking into consideration the sharpness of the Kikuchi lines additional information is obtained on the density of lattice defects.

6. REFERENCES

- [1] Bunge H J (1965) *Z. Metallk.* **56**: 872.
- [2] <http://www.eserc.stonybrook.edu/ProjectJava/Bragg>.
- [3] <http://www.isteam.univ-montp2.fr/TECTONOPHY/EBSD/EBSD-intro.html>.